

Propagation properties of Laguerre-Gaussian correlated Schell-model beam in non-Kolmogorov turbulence

Yuan Zhou,¹ Yangsheng Yuan,¹ Jun Qu,^{1,*} and Wei Huang^{2,3}

¹Department of Physics, Anhui Normal University, Wuhu, Anhui, 241000, China

²Laboratory of Atmospheric Physico-Chemistry, Anhui Institute of Optics & Fine Mechanics, Chinese Academy of Sciences, Hefei, Anhui 230031, China

³huangwei6@ustc.edu.cn

*qujun70@mail.ahnu.edu.cn

Abstract: Analytical formulas are derived for the average intensity, the root-mean-square (rms) angular width, and the M^2 -factor of Laguerre-Gaussian correlated Schell-model (LGCSM) beam propagating in non-Kolmogorov turbulence. The influence of the beam and turbulence parameters on the LGCSM beam is numerically calculated. It is shown that the quality of the LGCSM beam can be improved by choosing appropriate beam or turbulence parameter values. It is also found that the LGCSM beam has advantage over the Gaussian Schell-model (GSM) beam for reducing the turbulence-induced degradation. Our results will have some theoretical reference value for optical communications.

©2016 Optical Society of America

OCIS codes: (010.1290) Atmospheric optics; (010.1300) Atmospheric propagation; (030.0030) Coherence and statistical optics.

References and links

1. M. S. Belen'kii, J. D. Barchers, S. J. Karis, C. L. Osmon, J. M. Brown II, and R. Q. Fugate, "Preliminary experimental evidence of anisotropy of turbulence and the effect of non-Kolmogorov turbulence on wavefront tilt statistics," *Proc. SPIE* **3762**, 396–406 (1999).
2. A. Zilberman, E. Golbraikh, and N. S. Kopeika, "Lidar studies of aerosols and non-Kolmogorov turbulence in the Mediterranean troposphere," *Proc. SPIE* **5987**(598702), 598702, 598702-12 (2005).
3. I. Toselli, L. C. Andrews, R. L. Phillips, and V. Ferrero, "Free-space optical system performance for laser beam propagation through non-Kolmogorov turbulence," *Opt. Eng.* **47**(2), 122 (2008).
4. Z. Mei and O. Korotkova, "Random sources generating ring-shaped beams," *Opt. Lett.* **38**(2), 91–93 (2013).
5. F. Wang, X. Liu, Y. Yuan, and Y. Cai, "Experimental generation of partially coherent beams with different complex degrees of coherence," *Opt. Lett.* **38**(11), 1814–1816 (2013).
6. R. Chen, L. Liu, S. Zhu, G. Wu, F. Wang, and Y. Cai, "Statistical properties of a Laguerre-Gaussian Schell-model beam in turbulent atmosphere," *Opt. Express* **22**(2), 1871–1883 (2014).
7. L. Guo, Y. Chen, L. Liu, and Y. Cai, "Propagation of a Laguerre-Gaussian correlated Schell-model beam beyond the paraxial approximation," *Opt. Commun.* **352**, 127–134 (2015).
8. J. Cang, P. Xiu, and X. Liu, "Propagation of Laguerre-Gaussian and Bessel-Gaussian Schell-model beams through paraxial optical systems in turbulent atmosphere," *Opt. Laser Technol.* **54**, 35–41 (2013).
9. Y. Chen and Y. Cai, "Generation of a controllable optical cage by focusing a Laguerre-Gaussian correlated Schell-model beam," *Opt. Lett.* **39**(9), 2549–2552 (2014).
10. Z. Zhu, L. Liu, F. Wang, and Y. Cai, "Evolution properties of a Laguerre-Gaussian correlated Schell-model beam propagating in uniaxial crystals orthogonal to the optical axis," *J. Opt. Soc. Am. A* **32**(3), 374–380 (2015).
11. S. G. Reddy, A. Kumar, S. Prabhakar, and R. P. Singh, "Experimental generation of ring-shaped beams with random sources," *Opt. Lett.* **38**(21), 4441–4444 (2013).
12. Y. Chen, L. Liu, F. Wang, C. Zhao, and Y. Cai, "Elliptical Laguerre-Gaussian correlated Schell-model beam," *Opt. Express* **22**(11), 13975–13987 (2014).
13. Y. Chen, F. Wang, C. Zhao, and Y. Cai, "Experimental demonstration of a Laguerre-Gaussian correlated Schell-model vortex beam," *Opt. Express* **22**(5), 5826–5838 (2014).
14. L. C. Andrews and R. L. Phillips, *Laser Beam Propagation through Random Media* (SPIE, 2005).
15. T. Shirai, A. Dogariu, and E. Wolf, "Mode analysis of spreading of partially coherent beams propagating through atmospheric turbulence," *J. Opt. Soc. Am. A* **20**(6), 1094–1102 (2003).
16. T. Shirai, A. Dogariu, and E. Wolf, "Directionality of Gaussian Schell-model beams propagating in atmospheric turbulence," *Opt. Lett.* **28**(8), 610–612 (2003).

17. E. Shechpakina and O. Korotkova, "Second-order statistics of stochastic electromagnetic beams propagating through non-Kolmogorov turbulence," *Opt. Express* **18**(10), 10650–10658 (2010).
18. I. S. Gradshteyn and I. M. Ryzhik, *Table of Integrals, Series, and Products* (Academic Press, 1994).
19. I. Kimel and L. R. Elias, "Relations between Hermite and Laguerre Gaussian modes," *IEEE J. Quantum Electron.* **29**(9), 2562–2567 (1993).
20. Y. Dan and B. Zhang, "Beam propagation factor of partially coherent flat-topped beams in a turbulent atmosphere," *Opt. Express* **16**(20), 15563–15575 (2008).
21. Z. Song, Z. Liu, K. Zhou, Q. Sun, and S. Liu, "Propagation factors of multi-sinc Schell-model beams in non-Kolmogorov turbulence," *Opt. Express* **24**(2), 1804–1813 (2016).

1. Introduction

During the past decades, the studies on properties of beams propagating in the turbulence are mainly based on Kolmogorov's power spectrum of refractive index fluctuations. In recent years, many theoretical and experimental studies have pointed out that sometimes the Kolmogorov's theory is unable to describe the statistical properties of atmospheric turbulence correctly [1,2]. Toselli introduced non-Kolmogorov power spectrum of refractive index fluctuations to theoretically address these issues [3]. This theoretical model can give a reasonable physical explanation for unusual atmospheric turbulence behaviors. Therefore, many scholars study the laser beams propagating in non-Kolmogorov turbulence, and hence many studies of laser beams propagating in non-Kolmogorov turbulence have appeared recently in the literature.

Recently, LGCSM beam was proposed theoretically [4] and generated experimentally [5]. The intensity distribution of LGCSM beam displays a Gaussian profile at the source plane, while the far-field intensity distribution exhibits a ring-shaped profile. Due to their important applications in optical trapping and free-space optical communications, LGCSM beam has attracted a great deal of attention [5–13]. Chen and associates studied statistical properties of LGCSM beam propagating in Kolmogorov turbulent atmosphere [6]. Guo et al. analyzed properties of LGCSM beam propagation beyond the paraxial approximation [7]. Cang and associates investigated propagation properties of LGCSM beam through paraxial optical systems in Kolmogorov turbulent atmosphere [8]. Chen et al. generated a controllable optical cage by focusing LGCSM beam [9]. However, to the best of our knowledge, the normalized intensity, the rms angular width, and the M^2 -factor of LGCSM beam propagating in non-Kolmogorov turbulence have not been reported.

In the present work, on the basis of the extended Huygens-Fresnel principle, the cross-spectral density function, and the second-order moments of the Wigner distribution function (WDF), we have derived the analytical formulas for the average intensity, the rms angular width, and the M^2 -factor of LGCSM beam propagating in non-Kolmogorov turbulence. The influences of beam and turbulence parameter values on the normalized intensity, the rms angular width, and the M^2 -factor of LGCSM beam in the non-Kolmogorov turbulence have been studied in detail. We have also compared propagation properties of LGCSM beam with those of GSM beam.

2. The average intensity of LGCSM beam propagating in non-Kolmogorov turbulence

In the Cartesian coordinate system, the cross-spectral density function of the LGCSM beam at the source plane ($z = 0$) can be expressed as [4]

$$W(\mathbf{\rho}'_1, \mathbf{\rho}'_2, 0) = \exp\left(-\frac{|\mathbf{\rho}'_1|^2 + |\mathbf{\rho}'_2|^2}{4\sigma^2} - \frac{|\mathbf{\rho}'_1 - \mathbf{\rho}'_2|^2}{2\delta^2}\right) L_n\left(\frac{|\mathbf{\rho}'_1 - \mathbf{\rho}'_2|^2}{2\delta^2}\right), \quad (1)$$

where $\mathbf{\rho}'_1 = (x'_1, y'_1)$ and $\mathbf{\rho}'_2 = (x'_2, y'_2)$ are two arbitrary position vector at the source plane, σ is the beam width, δ is the transverse coherence width, and L_n is Laguerre polynomial of mode orders n .

Based on the extended Huygens-Fresnel principle [14], the cross-spectral density function of LGCSM beam at propagation distance z is

$$W(\boldsymbol{\rho}_1, \boldsymbol{\rho}_2, z) = \frac{k^2}{4\pi^2 z^2} \int_{-\infty}^{\infty} \int_{-\infty}^{\infty} \int_{-\infty}^{\infty} W(\boldsymbol{\rho}'_1, \boldsymbol{\rho}'_2, 0) \exp\left[-\frac{ik}{2z}(\boldsymbol{\rho}'_1 - \boldsymbol{\rho}_1)^2 + \frac{ik}{2z}(\boldsymbol{\rho}'_2 - \boldsymbol{\rho}_2)^2\right] \times \exp\left\langle \Psi(\boldsymbol{\rho}'_1, \boldsymbol{\rho}_1) + \Psi^*(\boldsymbol{\rho}'_2, \boldsymbol{\rho}_2) \right\rangle d^2 \boldsymbol{\rho}'_1 d^2 \boldsymbol{\rho}'_2, \quad (2)$$

where $k = 2\pi/\lambda$ represents the wave number with the wavelength λ , $\boldsymbol{\rho}_1$ and $\boldsymbol{\rho}_2$ are two arbitrary position vectors at the output plane, Ψ denotes the random part of the complex phase of a spherical wave propagating in the turbulence from the source plane to the output plane, and the notations $*$ and $\langle \rangle$ indicate the complex conjugate and the ensemble average, respectively. Equation (2) represents the average intensity at the output plane when $\boldsymbol{\rho}_1 = \boldsymbol{\rho}_2 = \boldsymbol{\rho}$. The last term in Eq. (2) can be expressed as [16]

$$\exp\left\langle \Psi(\boldsymbol{\rho}'_1, \boldsymbol{\rho}) + \Psi^*(\boldsymbol{\rho}'_2, \boldsymbol{\rho}) \right\rangle = \exp\left\{ -4\pi^2 k^2 z \int_0^1 \int_0^{\infty} \kappa \Phi_n(\kappa, \alpha) [1 - J_0(\kappa \xi |\boldsymbol{\rho}'_1 - \boldsymbol{\rho}'_2|)] d\kappa d\xi \right\}, \quad (3)$$

where J_0 is the Bessel function of zero order and can be approximated as [15]

$$J_0(\kappa \xi |\boldsymbol{\rho}'_1 - \boldsymbol{\rho}'_2|) \sim 1 - \frac{1}{4} (\kappa \xi |\boldsymbol{\rho}'_1 - \boldsymbol{\rho}'_2|)^2, \quad (4)$$

$\Phi_n(\kappa, \alpha)$ is the spatial power spectrum of the refractive-index fluctuations of the turbulent medium, and κ is the two-dimensional spatial frequency. According to the non-Kolmogorov turbulence theory, $\Phi_n(\kappa, \alpha)$ can be expressed as [3, 16, 17]

$$\Phi_n(\kappa, \alpha) = A(\alpha) \tilde{C}_n^2 \frac{\exp\left[-\left(\kappa^2/\kappa_m^2\right)\right]}{\kappa^2 + \kappa_0^2}, \quad 0 \leq \kappa < \infty, 3 < \alpha < 4. \quad (5)$$

Here, α denotes the power-law exponent ($3 < \alpha < 4$), $\kappa_0 = 2\pi/L_0$ (L_0 denotes the outer scale of turbulence), $\kappa_m = c(\alpha)/l_0$ (l_0 denotes the inner scale of turbulence), and

$$c(\alpha) = \left[\Gamma(5 - \alpha/2) \cdot A(\alpha) \cdot 2\pi/3 \right]^{1/(\alpha-5)}, \quad (6)$$

$$A(\alpha) = \Gamma(\alpha - 1) \cdot \cos(\alpha\pi/2) / 4\pi^2, \quad (7)$$

where \tilde{C}_n^2 is a generalized refractive index structure parameter with units $m^{3-\alpha}$. The spectrum expressed in Eq. (5) reduces to Kolmogorov spectrum when $\alpha = 11/3$, $L_0 = \infty$, $l_0 = 0$ and $\tilde{C}_n^2 = C_n^2$.

Substituting Eq. (4) into (3), we obtain

$$\exp\left\langle \Psi(\boldsymbol{\rho}'_1, \boldsymbol{\rho}) + \Psi^*(\boldsymbol{\rho}'_2, \boldsymbol{\rho}) \right\rangle = \exp\left(-\frac{1}{3} \pi^2 k^2 z |\boldsymbol{\rho}'_1 - \boldsymbol{\rho}'_2|^2 T\right), \quad (8)$$

where T can be expressed as [3, 16, 17]

$$T = \int_0^{\infty} \kappa^3 \Phi_n(\kappa, \alpha) d\kappa = \frac{A(\alpha) \tilde{C}_n^2 \kappa_m^{2-\alpha} \beta \exp\left(\frac{\kappa_0^2}{\kappa_m^2}\right) \Gamma\left(2 - \frac{\alpha}{2}, \frac{\kappa_0^2}{\kappa_m^2}\right) - 2\kappa_0^{4-\alpha}}{2(\alpha - 2)}, \quad (9)$$

where $\beta = 2\kappa_0^2 - 2\kappa_m^2 + \alpha\kappa_m^2$, and Γ is the incomplete Gamma function.

If $\rho_1 = \rho_2 = \rho = (x, y)$, substituting Eqs. (1), (8) and (9) into Eq. (2) leads to the analytical formulas for the average intensity of LGCSM beam propagating in non-Kolmogorov turbulence through complex operation (see Appendix for the derivation)

$$\begin{aligned}
 I(x, y, z) &= W(\rho, \rho, z) \\
 &= \frac{k^2}{4z^2} \sum_{g=0}^n \sum_{h=0}^{2g} \sum_{j=0}^{2n-2g} \sum_{m=0}^{2g-h} \sum_{p=0}^{2n-2g-j} \sum_{s=0}^{\lfloor \frac{h}{2} \rfloor} \sum_{t=0}^{\lfloor \frac{m}{2} \rfloor} \sum_{u=0}^{\lfloor \frac{j}{2} \rfloor} \sum_{v=0}^{\lfloor \frac{p}{2} \rfloor} \binom{n}{g} \binom{2g}{h} \binom{2n-2g}{j} \binom{2g-h}{m} \binom{2n-2g-j}{p} \\
 &\times (-1)^{h-s+t+j-u+v+n} 2^{\frac{h-2n+j}{2}-3n} i^{-h+2s-m+2t-j+2u-p+2v} \delta^{-h+2s-j+2u} f_3^{m-2t+p-2v} \\
 &\times f_4^{\frac{-h+2s-m+2t-j+2u-p+2v-2}{2}} \frac{1}{f_1} \left(1 - \frac{1}{f_1 \delta^2}\right)^{\frac{2g-h+2n-2g-j}{2}} \frac{1}{n!} \frac{h!}{s!(h-2s)!} \frac{m!}{t!(m-2t)!} \frac{j!}{u!(j-2u)!} \quad (10) \\
 &\times \frac{p!}{v!(p-2v)!} \exp\left[\left(-\frac{k^2}{4f_1 z^2} + \frac{f_5^2}{4f_4}\right)(x^2 + y^2)\right] H_{h-2s+m-2t}\left(\frac{if_3 x}{2\sqrt{f_4}}\right) H_{j-2u+p-2v}\left(\frac{if_3 y}{2\sqrt{f_4}}\right) \\
 &\times H_{2g-h-m}\left(\frac{ikx}{z\sqrt{2}\sqrt{f_1^2 \delta^2 - f_1}}\right) H_{2n-2g-j-p}\left(\frac{iky}{z\sqrt{2}\sqrt{f_1^2 \delta^2 - f_1}}\right),
 \end{aligned}$$

where

$$\begin{aligned}
 f_1 &= \frac{1}{4\sigma^2} + \frac{1}{2\delta^2} + \frac{ik}{2z} + \frac{\pi^2 k^2 zT}{3}, f_2 = \frac{1}{\delta^2} + \frac{2}{3} \pi^2 k^2 zT, f_3 = \frac{f_2}{\sqrt{2}\sqrt{f_1^2 \delta^2 - f_1}}, \\
 f_4 &= \frac{1}{4\sigma^2} + \frac{1}{2\delta^2} - \frac{ik}{2z} + \frac{\pi^2 k^2 zT}{3} - \frac{f_2^2}{4f_1}, f_5 = \frac{ikf_2}{2f_1 z} - \frac{ik}{z}.
 \end{aligned} \quad (11)$$

The following integral formula has been used in the derivation of the above Eq. (10) [18, 19].

$$L_n^m(\rho^2) = \frac{(-1)^n}{2^{2n} n!} \sum_{r=0}^n \binom{n}{r} H_{2r}(x) H_{2(n-r)}(y), \quad (12)$$

$$H_n(x+y) = 2^{-\frac{n}{2}} \sum_{k=0}^n \binom{n}{k} H_{n-k}(\sqrt{2}x) H_k(\sqrt{2}y), \quad (13)$$

$$\int_{-\infty}^{\infty} \exp[-(x-y)^2] H_n(\alpha x) dx = \sqrt{\pi} (1-\alpha^2)^{\frac{n}{2}} H_n\left(\frac{\alpha y}{\sqrt{1-\alpha^2}}\right), \quad (14)$$

$$H_n(x) = \sum_{k=0}^{\lfloor \frac{n}{2} \rfloor} \frac{(-1)^k n!}{k!(n-2k)!} (2x)^{n-2k}, \quad (15)$$

$$\int_{-\infty}^{\infty} x^n \exp[-(x-b)^2] dx = (2i)^{-n} \sqrt{\pi} H_n(ib). \quad (16)$$

3. Second-order moments of LGCSM beam in non-Kolmogorov turbulence

The cross-spectral density function of LGCSM beam at the source plane can be expressed in Eq. (1). For the convenience of the calculation, the following “sum” and “difference” coordinates are applied to Eq. (2)

$$\boldsymbol{\rho}' = \frac{\boldsymbol{\rho}_1 + \boldsymbol{\rho}_2}{2}, \boldsymbol{\rho}'_d = \boldsymbol{\rho}'_1 - \boldsymbol{\rho}'_2, \boldsymbol{\rho} = \frac{\boldsymbol{\rho}_1 + \boldsymbol{\rho}_2}{2}, \boldsymbol{\rho}_d = \boldsymbol{\rho}_1 - \boldsymbol{\rho}_2. \quad (17)$$

Equation (2) can then be written as

$$W(\boldsymbol{\rho}, \boldsymbol{\rho}_d, z) = \left(\frac{k}{2\pi z}\right)^2 \int_{-\infty}^{\infty} \int_{-\infty}^{\infty} W(\boldsymbol{\rho}', \boldsymbol{\rho}'_d, 0) \exp\left\{\frac{ik}{z}[(\boldsymbol{\rho} - \boldsymbol{\rho}') \cdot (\boldsymbol{\rho}_d - \boldsymbol{\rho}'_d)] - H(\boldsymbol{\rho}_d, \boldsymbol{\rho}'_d, z)\right\} d^2\boldsymbol{\rho}' d^2\boldsymbol{\rho}'_d, \quad (18)$$

where $H(\boldsymbol{\rho}_d, \boldsymbol{\rho}'_d, z)$ represents the effect of non-Kolmogorov turbulence.

After some operations as shown in [20], Eq. (18) can be expressed as

$$W(\boldsymbol{\rho}, \boldsymbol{\rho}_d, z) = \left(\frac{1}{2\pi}\right)^2 \int_{-\infty}^{\infty} \int_{-\infty}^{\infty} W\left(\boldsymbol{\rho}^*, \boldsymbol{\rho}_d + \frac{z}{k}\boldsymbol{\kappa}_d, 0\right) d^2\boldsymbol{\rho}^* d^2\boldsymbol{\kappa}_d \times \exp\left[-i\boldsymbol{\rho} \cdot \boldsymbol{\kappa}_d + i\boldsymbol{\rho}^* \cdot \boldsymbol{\kappa}_d - \frac{\pi^2 k^2 z}{3} \left(\frac{z^2}{k^2} \boldsymbol{\kappa}_d^2 + 3\frac{z}{k} \boldsymbol{\kappa}_d \boldsymbol{\rho}_d + 3\boldsymbol{\rho}_d^2\right) T\right], \quad (19)$$

where $\boldsymbol{\kappa}_d$ is the position vector in the spatial-frequency domain, and the cross-spectral density function $W\left(\boldsymbol{\rho}^*, \boldsymbol{\rho}_d + \frac{z}{k}\boldsymbol{\kappa}_d, 0\right)$ can be expressed as [6]

$$W\left(\boldsymbol{\rho}^*, \boldsymbol{\rho}_d + \frac{z}{k}\boldsymbol{\kappa}_d, 0\right) = \exp\left[-\frac{1}{2\sigma^2} \boldsymbol{\rho}^{*2} - \left(\frac{1}{8\sigma^2} + \frac{1}{2\delta^2}\right) \left(\boldsymbol{\rho}_d + \frac{z}{k}\boldsymbol{\kappa}_d\right)^2\right] L_n\left[\frac{1}{2\delta^2} \left(\boldsymbol{\rho}_d + \frac{z}{k}\boldsymbol{\kappa}_d\right)^2\right]. \quad (20)$$

The WDF of partially coherent beam can be expressed in terms of the cross-spectral density function $W(\boldsymbol{\rho}, \boldsymbol{\rho}_d, z)$ as [20, 21]

$$h(\boldsymbol{\rho}, \boldsymbol{\theta}, z) = \left(\frac{k}{2\pi}\right)^2 \int_{-\infty}^{\infty} W(\boldsymbol{\rho}, \boldsymbol{\rho}_d, z) \exp(-ik\boldsymbol{\theta} \cdot \boldsymbol{\rho}_d) d^2\boldsymbol{\rho}_d, \quad (21)$$

where vector $\boldsymbol{\theta} = (\theta_x, \theta_y)$ denotes an angle which the vector of interest makes with the z -direction, $k\theta_x$ and $k\theta_y$ are the wave vector components along the x - and y -axis, respectively.

Substituting Eqs. (19) and (20) into Eq. (21), the WDF of LGCSM beam in non-Kolmogorov turbulence can be expressed as

$$h(\boldsymbol{\rho}, \boldsymbol{\theta}, z) = \frac{k^2}{16\pi^4} 2\pi\sigma^2 \int_{-\infty}^{\infty} \int_{-\infty}^{\infty} L_n\left[\frac{1}{2\delta^2} \left(\boldsymbol{\rho}_d + \frac{z}{k}\boldsymbol{\kappa}_d\right)^2\right] \times \exp(-a\boldsymbol{\rho}_d^2 - b\boldsymbol{\kappa}_d^2 - c\boldsymbol{\rho}_d \cdot \boldsymbol{\kappa}_d - ik\boldsymbol{\theta} \cdot \boldsymbol{\rho}_d - i\boldsymbol{\rho} \cdot \boldsymbol{\kappa}_d) d^2\boldsymbol{\kappa}_d d^2\boldsymbol{\rho}_d, \quad (22)$$

where

$$a = \frac{1}{8\sigma^2} + \frac{1}{2\delta^2} + \pi^2 k^2 z T, b = \frac{z^2}{8k^2 \sigma^2} + \frac{z^2}{2k^2 \delta^2} + \frac{\sigma^2}{2} + \frac{\pi^2 z^3 T}{3}, c = \frac{z}{4k\sigma^2} + \frac{z}{k\delta^2} + \pi^2 k z^2 T. \quad (23)$$

The moments of order $n_1 + n_2 + m_1 + m_2$ of the WDF of a beam is defined as [21]

$$\langle x^{n_1} y^{n_2} \theta_x^{m_1} \theta_y^{m_2} \rangle = \frac{1}{P} \int_{-\infty}^{\infty} \int_{-\infty}^{\infty} x^{n_1} y^{n_2} \theta_x^{m_1} \theta_y^{m_2} h(\boldsymbol{\rho}, \boldsymbol{\theta}, z) d^2 \boldsymbol{\rho} d^2 \boldsymbol{\theta}, \quad (24)$$

where

$$P = \int_{-\infty}^{\infty} \int_{-\infty}^{\infty} h(\boldsymbol{\rho}, \boldsymbol{\theta}, z) d^2 \boldsymbol{\rho} d^2 \boldsymbol{\theta}. \quad (25)$$

Substituting Eqs. (22), (23) and (25) into Eq. (24), the analytical formulas for the second-order moments of the WDF of LGCSM beam propagating through non-Kolmogorov turbulence can be derived as

$$\langle \boldsymbol{\rho}^2 \rangle = \frac{z^2}{k^2} \left[\frac{1}{2\sigma^2} + \frac{2}{\delta^2} (1+n) \right] + 2\sigma^2 + \frac{4\pi^2 z^3 T}{3}, \quad (26)$$

$$\langle \boldsymbol{\theta}^2 \rangle = \frac{1}{k^2} \left[\frac{1}{2\sigma^2} + \frac{2}{\delta^2} (1+n) \right] + 4\pi^2 z T, \quad (27)$$

$$\langle \boldsymbol{\rho} \cdot \boldsymbol{\theta} \rangle = -\frac{z}{k^2} \left[\frac{1}{2\sigma^2} + \frac{2}{\delta^2} (1+n) \right] - 2\pi^2 z^2 T. \quad (28)$$

According to Eqs. (26)-(28), the rms angular width and the M^2 -factor of LGCSM beam propagating in non-Kolmogorov turbulence can be obtained as

$$\theta_N(z) \equiv \left(\langle |\boldsymbol{\theta} - \langle \boldsymbol{\theta} \rangle|^2 \rangle \right)^{1/2} = \left(\langle \boldsymbol{\theta}^2 \rangle \right)^{1/2} = \left\{ \frac{1}{k^2} \left[\frac{1}{2\sigma^2} + \frac{2}{\delta^2} (1+n) \right] + 4\pi^2 z T \right\}^{1/2}, \quad (29)$$

$$\begin{aligned} M^2(z) &= k \left(\langle \boldsymbol{\rho}^2 \rangle \langle \boldsymbol{\theta}^2 \rangle - \langle \boldsymbol{\rho} \cdot \boldsymbol{\theta} \rangle^2 \right)^{1/2} \\ &= k \left\{ \left[\frac{z^2}{2k^2 \sigma^2} + \frac{2z^2}{k^2 \delta^2} (1+n) + 2\sigma^2 + \frac{4\pi^2 z^3 T}{3} \right] \left[\frac{1}{2k^2 \sigma^2} + \frac{2}{k^2 \delta^2} (1+n) + 4\pi^2 z T \right] \right. \\ &\quad \left. - \left[\frac{z}{2k^2 \sigma^2} + \frac{2z}{k^2 \delta^2} (1+n) + 2\pi^2 z^2 T \right]^2 \right\}^{1/2}. \quad (30) \end{aligned}$$

4. Numerical results and analysis

According to Eq. (10), we have made an analysis about the average intensity of LGCSM beam propagating in non-Kolmogorov turbulence, and the results are shown in Figs. 1 and 2.

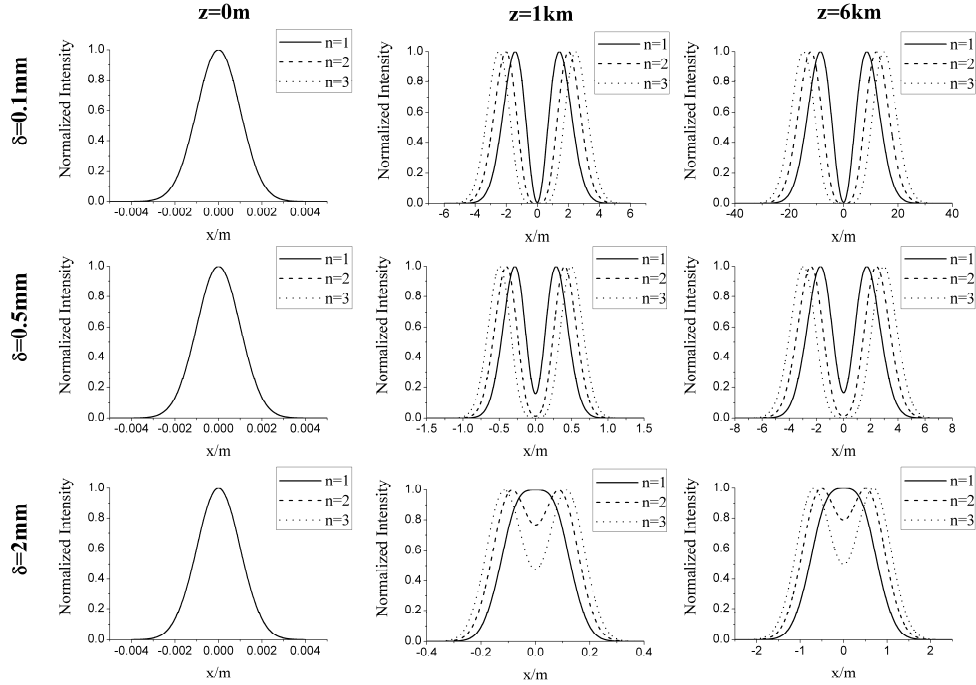


Fig. 1. The normalized intensity of LGCSM beam with different mode order n and transverse coherence width δ in non-Kolmogorov turbulence at several propagation distances. The calculation parameters are: $\tilde{C}_n^2 = 10^{-14} m^{-3-\alpha}$, $\lambda = 632.8nm$, $\sigma = 1mm$, $\kappa = 10$, $\alpha = 3.8$, $L_0 = 1m$, and $l_0 = 0.01m$.

Figure 1 shows that the intensity distribution of LGCSM beam at the source plane has a Gaussian beam profile. With the increase of propagation distance, the LGCSM beam converts to a hollow profile, and the larger mode order n or the smaller transverse coherence width δ of the beam, the quicker will be the conversion. In Fig. 2, one can see that the normalized intensity distribution of LGCSM beam propagating in non-Kolmogorov turbulence converts to Gaussian profile, and the conversion is quicker with smaller power-law exponent α and inner scale l_0 , or larger outer scale L_0 and structure constant \tilde{C}_n^2 . This means that the intensity distribution of LGCSM beam propagating in non-Kolmogorov turbulence is more affected by the strength of turbulence.

According to Eqs. (29) and (30), we have also analyzed the rms angular width and the M^2 -factor of LGCSM beam propagating in non-Kolmogorov turbulence. Figure 3 shows the normalized rms angular width of LGCSM beams with different mode order propagating in non-Kolmogorov turbulence. Under the condition of $n = 0$, the LGCSM beam reduces to the GSM beam. From Fig. 3, one finds that the normalized rms angular width of LGCSM beam increases with the propagation distance in the turbulence. Meanwhile, the beam with a larger mode order has a smaller rms angular width, and thus is less affected by the non-Kolmogorov turbulence.

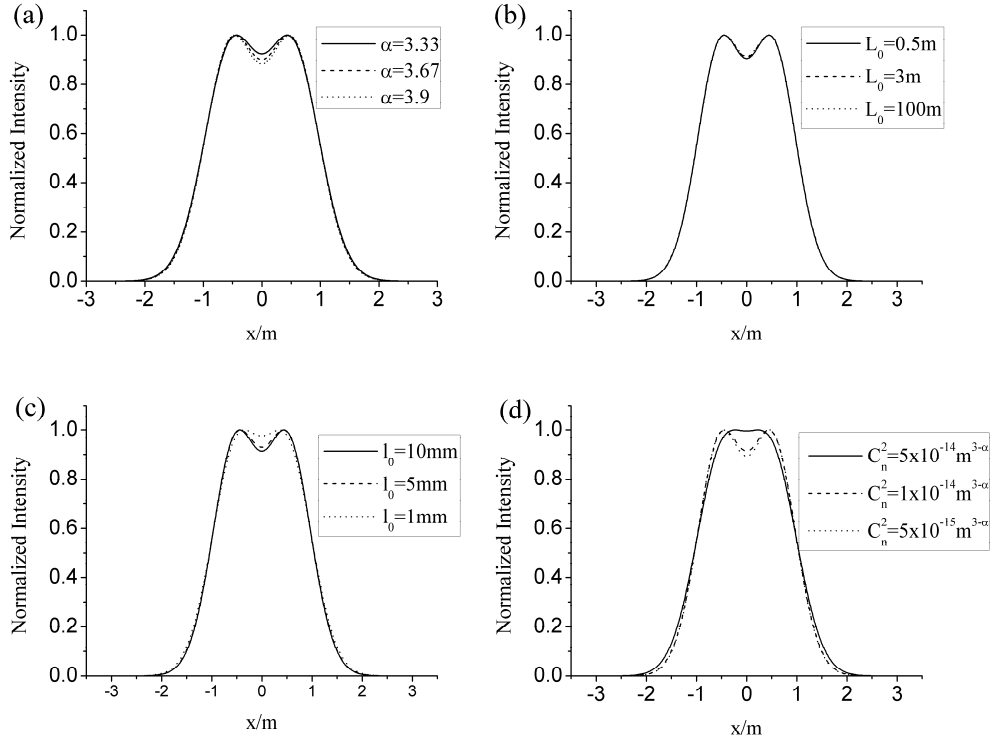


Fig. 2. The normalized intensity of LGCSM beam in non-Kolmogorov turbulence at propagation distance $z = 6\text{km}$ for different power-law exponent α , outer scale L_0 , inner scale l_0 , and structure constant \tilde{C}_n^2 . The calculation parameters are: $n = 1$, and $\delta = 1.5\text{mm}$. (a) $\tilde{C}_n^2 = 10^{-14} \text{m}^{3-\alpha}$, $L_0 = 1\text{m}$, and $l_0 = 0.01\text{m}$. (b) $\tilde{C}_n^2 = 10^{-14} \text{m}^{3-\alpha}$, $\alpha = 3.8$, and $l_0 = 0.01\text{m}$. (c) $\tilde{C}_n^2 = 10^{-14} \text{m}^{3-\alpha}$, $\alpha = 3.8$, and $L_0 = 1\text{m}$. (d) $\alpha = 3.8$, $L_0 = 1\text{m}$, and $l_0 = 0.01\text{m}$.

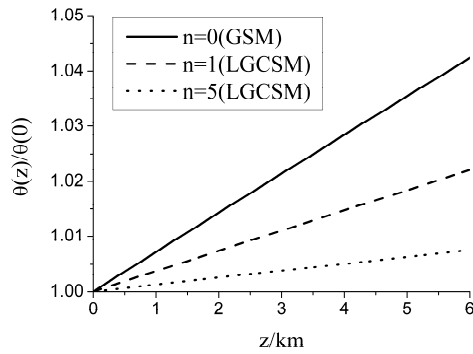


Fig. 3. The normalized rms angular width of LGCSM beams propagating in non-Kolmogorov turbulence with different mode order n . The calculation parameters are: $\tilde{C}_n^2 = 10^{-15} \text{m}^{3-\alpha}$, $\lambda = 632.8\text{nm}$, $\sigma = 0.01\text{m}$, $\delta = 0.005\text{m}$, $\kappa = 10$, $\alpha = 3.8$, $L_0 = 1\text{m}$, and $l_0 = 0.01\text{m}$.

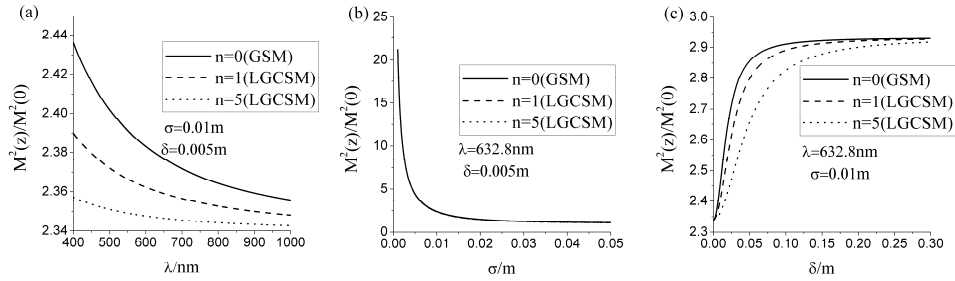


Fig. 4. The normalized M^2 -factor of LGCSM beam at propagation distance $z = 6\text{km}$ in non-Kolmogorov turbulence as a function of (a) wavelength λ , (b) beam width σ , and (c) transverse coherence width δ .

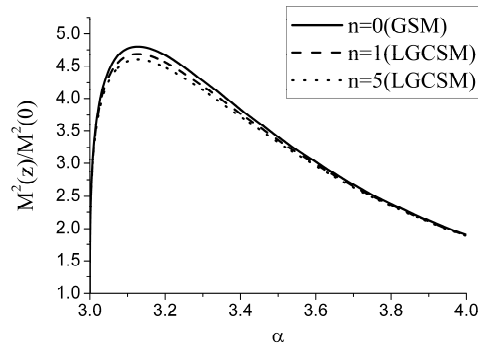


Fig. 5. The normalized M^2 -factor of LGCSM beam at propagation distance $z = 6\text{km}$ in non-Kolmogorov turbulence as a function of α .

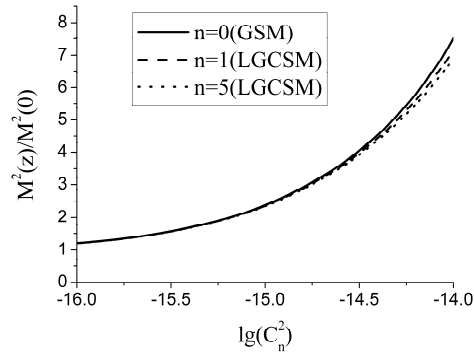


Fig. 6. The normalized M^2 -factor of LGCSM beam at propagation distance $z = 6\text{km}$ in non-Kolmogorov turbulence as a function of \tilde{C}_n^2 .

In Figs. 4-6, the parameters are the same as in Fig. 3. Figures 4-6 show the variations of the normalized M^2 -factor of LGCSM beam with the beam or turbulence parameter values at propagation distance $z = 6\text{km}$ in non-Kolmogorov turbulence. Figures 4(a) and 4(b) give that the normalized M^2 -factor decreases with the increase of the wavelength λ and the beam width σ . Figure 4(c) indicates that the M^2 -factor increases with the increase of transverse coherence width δ . This means that LGCSM beam with a larger mode order n , a longer wavelength λ , a larger beam width σ , or a smaller transverse coherence width δ is less affected by non-

Kolmogorov turbulence. Figure 5 shows that the normalized M^2 -factor of LGCSM beams with different mode orders all reach the maximum value when $\alpha = 3.128$. The normalized M^2 -factor increases (decreases) with the value of α when $\alpha < (>) 3.128$, which means that the LGCSM beam is more affected by stronger non-Kolmogorov turbulence. Figure 6 shows that the normalized M^2 -factor increases with the parameter \tilde{C}_n^2 . In addition, one can also find from Figs. 4-6 that the LGCSM beam with larger mode order n is less affected by the non-Kolmogorov turbulence.

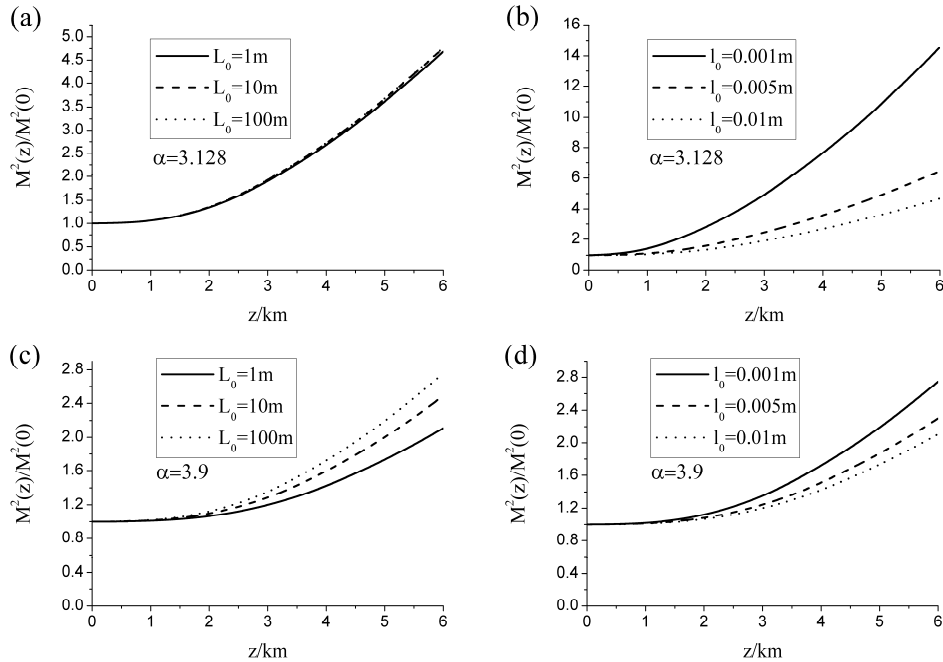


Fig. 7. The normalized M^2 -factor of LGCSM beam with mode order $n = 1$ propagating in non-Kolmogorov turbulence for different power-law exponent α , outer scale L_0 and inner scale l_0 .

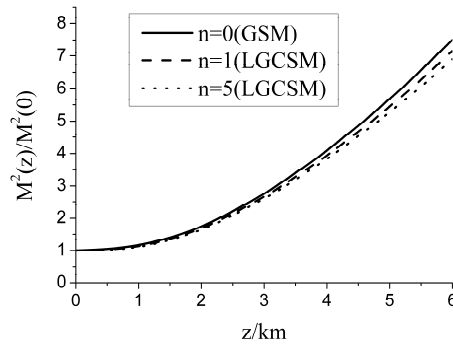


Fig. 8. The normalized M^2 -factor of LGCSM beams with different mode order propagating in non-Kolmogorov turbulence.

Figure 7 shows the changes of the normalized M^2 -factor with the z value for LGCSM beam with mode order $n = 1$ propagating in non-Kolmogorov turbulence with different power-law exponent α , outer scale L_0 , and inner scale l_0 . The other parameters are the same

as in Fig. 3. The turbulence with $\alpha = 3.128$ is stronger than the turbulence with $\alpha = 3.9$. From Figs. 7(a) and 7(c), one finds that the normalized M^2 -factor of LGCSM beam increases with the increase of outer scale L_0 , and it is not sensitive to the change of L_0 under the condition of strong turbulence [see Fig. 7(a)]. Figures 7(b) and 7(d) shows that the normalized M^2 -factor of LGCSM beam decreases with the increase of inner scale l_0 . It can also be seen from Fig. 7 that the LGCSM beam is less affected by the non-Kolmogorov turbulence when the outer scale L_0 becomes smaller or the inner scale l_0 becomes larger.

Figure 8 compares the normalized M^2 -factor of LGCSM beam and GSM beam propagating in non-Kolmogorov turbulence. In this figure, we set $\tilde{C}_n^2 = 10^{-14} m^{3-\alpha}$, and other parameter values are the same as those used in Fig. 3. The figure shows that the normalized M^2 -factors of LGCSM beams are smaller than GSM beams, meaning that the former beams are less affected by non-Kolmogorov turbulence than the latter beams.

5. Conclusions

Based on the extended Huygens-Fresnel principle, the cross-spectral density function and the second-order moments of the Wigner distribution function (WDF), we have derived the analytical formulas for the average intensity, the rms angular width, and the M^2 -factor of LGCSM beam propagating in non-Kolmogorov turbulence. The effect of beam parameters and turbulence strength on the average intensity, the rms angular width, and the M^2 -factor of LGCSM beam has been analyzed. It is found that the quality of LGCSM beam can be improved by choosing a larger mode order n , longer wavelength λ , larger beam width σ or smaller transverse coherence width δ . And the LGCSM will be less affected by weak turbulence, such as the turbulence with larger power-law exponent α or larger inner scale l_0 or smaller outer scale L_0 or smaller generalized refractive index structure parameter \tilde{C}_n^2 . Besides, the LGCSM beam is significantly less affected by non-Kolmogorov turbulence compared with GSM beam. Our results will have some reference value for optical communication.

6. Appendix: the derivation of Eq. (10)

While $\mathbf{p}_1 = \mathbf{p}_2 = \mathbf{p} = (x, y)$, substituting Eqs. (1), (8) and (9) into Eq. (2). The analytical formulas for the average intensity of LGCSM beam propagating in non-Kolmogorov turbulence can be expressed as

$$\begin{aligned}
 I(x, y, z) &= W(\mathbf{p}, \mathbf{p}, z) \\
 &= \frac{k^2}{4\pi^2 z^2} \int \int \int \int \exp \left[-\frac{(x_1^2 + y_1^2) + (x_2^2 + y_2^2)}{4\sigma^2} - \frac{(x_1' - x_2')^2 + (y_1' - y_2')^2}{2\delta^2} \right] \\
 &\times \exp \left\{ -\frac{ik}{2z} [(x_1' - x)^2 + (y_1' - y)^2] + \frac{ik}{2z} [(x_2' - x)^2 + (y_2' - y)^2] \right\} L_n \left(\frac{(x_1' - x_2')^2 + (y_1' - y_2')^2}{2\delta^2} \right) \\
 &\times \exp \left\{ -\frac{1}{3} \pi^2 k^2 z T [(x_1' - x_2')^2 + (y_1' - y_2')^2] \right\} dx_1' dx_2' dy_1' dy_2'.
 \end{aligned} \tag{31}$$

With the help of Eqs. (12) and (13), Eq. (31) can be expressed as

$$\begin{aligned}
I(x, y, z) &= W(\boldsymbol{\rho}, \boldsymbol{\rho}, z) \\
&= \frac{k^2}{4\pi^2 z^2} \int_{-\infty}^{\infty} \int_{-\infty}^{\infty} dx'_2 dy'_2 \sum_{g=0}^n \sum_{h=0}^{2g} \sum_{j=0}^{2n-2g} \binom{n}{g} \binom{2g}{h} \binom{2n-2g}{j} \frac{(-1)^n}{2^{2n} n!} H_h\left(\frac{-x'_2}{\delta}\right) H_j\left(\frac{-y'_2}{\delta}\right) \\
&\times \exp\left(-\frac{x'^2_2 + y'^2_2}{4\sigma^2} + \frac{-x'^2_2 - y'^2_2}{2\delta^2}\right) \exp\left[\frac{ik}{2z}(x'^2_2 - 2x'_2 x + y'_2 - 2y'_2 y)\right] \exp\left[\frac{1}{3}\pi^2 k^2 z T(-x'^2_2 - y'^2_2)\right] \\
&\times \int_{-\infty}^{\infty} H_{2g-h}\left(\frac{x'_1}{\delta}\right) \exp\left[-f_1 x'^2_1 + \left(f_2 x'_2 + \frac{ikx}{z}\right)x'_1\right] dx'_1 \\
&\times \int_{-\infty}^{\infty} H_{2n-2g-j}\left(\frac{y'_1}{\delta}\right) \exp\left[-f_1 y'^2_1 + \left(f_2 y'_2 + \frac{iky}{z}\right)y'_1\right] dy'_1.
\end{aligned} \tag{32}$$

where f_1 and f_2 are defined in Eq. (11). With the help of Eq. (14), we calculating the integral with respect to x'_1 and y'_1 , and substituting the answers into Eq. (32). Thus, Eq. (32) can be expressed as

$$\begin{aligned}
I(x, y, z) &= W(\boldsymbol{\rho}, \boldsymbol{\rho}, z) \\
&= \frac{k^2}{4\pi^2 z^2} \sum_{g=0}^n \sum_{h=0}^{2g} \sum_{m=0}^{2n-2g} \sum_{p=0}^{2n-2g-j} \binom{n}{g} \binom{2g}{h} \binom{2n-2g}{j} \binom{2g-h}{m} \binom{2n-2g-j}{p} 2^{\frac{-h+2n-j}{2}-3n} \\
&\times \frac{1}{f_1} \frac{(-1)^n}{n!} \left(1 - \frac{1}{f_1 \delta^2}\right)^{\frac{-h+2n-j}{2}} \exp\left[-\frac{k^2}{4f_1 z^2}(x^2 + y^2)\right] H_{2g-h-m}\left(\frac{ikx}{z\sqrt{2}\sqrt{f_1^2 \delta^2 - f_1}}\right) \\
&\times H_{2n-2g-j-p}\left(\frac{iky}{z\sqrt{2}\sqrt{f_1^2 \delta^2 - f_1}}\right) \int_{-\infty}^{\infty} H_h\left(\frac{-x'_2}{\delta}\right) H_m(f_3 x'_2) \exp[-f_4 x'^2_2 + f_5 x x'_2] dx'_2 \\
&\times \int_{-\infty}^{\infty} H_j\left(\frac{-y'_2}{\delta}\right) H_p(f_3 y'_2) \exp[-f_4 y'^2_2 + f_5 y y'_2] dy'_2.
\end{aligned} \tag{33}$$

where f_3, f_4 and f_5 are defined in Eq. (11). With the help of Eqs. (15) and (16), we calculating the integral with respect to x'_2 and y'_2 , and substituting the answers into Eq. (33). Thus, the analytical formulas for the average intensity of LGCSM beam propagating in non-Kolmogorov turbulence can be expressed as Eq. (10).

Acknowledgments

This work is supported by the National Natural Science Foundation of China (NSFC) under Grants Nos. 11374015, 21133008, and 11404007.